Structure and Room Temperature Ferromagnetism of Ni $^{2+}$- doped ZnO Thin film Prepared by Sol-gel Process

Trilok Kumar Pathak[1], Prabha Singh[2], L.P.Purohit[3]

[1,3]Department of Physics, Gurukul Kangri Vishwavidyalaya, Haridwar (U.K.)-India

[2]Department of Physics, Vira college of Engineering, Bijnor (U.P.)-India

(tpathak01@gmail.com, prabhasingh07@gmail.com, lppurohit@gmail.com)

Abstract- In this study, Ni doped ZnO ($Zn_{1-x}Ni_xO$, x= 0.02, 0.04, 0.07) Diluted magnetic semiconductors (DMSs) thin films onto Si substrates by spin-coating method from a precursor solution containing zinc acetate dissolved in methanol. After deposition, these films were preheated at 350^0C for five minute and then annealed at 550^0C for three hour for crystallize. Scanning Electron microscopy (SEM) image shows the particle size with an average size of 250 nm. The analysis of X-ray diffraction (XRD) identified that the impurity phase is observed when the Ni content x reaches 0.07. With the increment of x, wurtzite structures degrade gradually. The magnetic properties are measured using Vibrating Sample Magnetometer (VSM) at room temperature; the $Zn_{1-x}Ni_xO$ (x=0.07) thin film shows ferromagnetism. The magnetic moment depends on Ni concentration and increases continuously as Ni concentration increases.

Keywords - ZnNiO thin films, Structure and ferromagnetism.

1. INTRODUCTION

ZnO has attracted considerable interest due to its potentials in optoelectronic applications. It has wide band gap (3.37 ev) and a large exciton binding energy (60 mev) [1]. Diluted magnetic semiconductors (DMSs) have recently attracted broad interest for their promise in generating and manipulating spin-polarized currents [2]. Optically transparent ferromagnetic DMSs, obtained by doping paramagnetic transition metal ions into wide band gap semiconductors, have received particular attention for integrated optospintronic applications [3,4]. Specifically, ZnO, which has large band gap and exciton binding energies, excellent mechanical characteristics, and is inexpensive and environmentally safe, has been identified as a promising host material. Stable ferromagnetic configurations arising from carrier-mediated exchange interactions have been predicted for several transition metal- doped ZnO DMSs [5,6]. Room-temperature ferromagnetism has been observed only for V^{2+}:ZnO [7], Fe^{2+}:ZnO [8], and Co^{2+}:ZnO [9,10]. Magnetic properties have been reported for otherwise similar films, indicating a strong dependence on synthesis and processing conditions. In some cases, even the conclusion of intrinsic ferromagnetism remains controversial. In this Letter, we report high-*Tc*

ferromagnetism in nano crystalline Ni^{2+}:ZnO prepared from solution at low temperatures. High-*Tc* ferromagnetism has not been reported previously for any Ni^{2+}-based DMS, and this discovery narrows the gap between theoretical predictions and experimental results. The appearance of ferromagnetism upon room-temperature aggregation of paramagnetic Ni^{2+}:ZnO DMS nano crystals unambiguously demonstrates its intrinsic origin and additionally represents a significant advance toward chemically controlled spin effects in semiconductor nanostructures. The sol-gel process has been successfully used to obtain nano scale material at low cost. In this work, the sol-gel process is developed to prepare ZnNiO nano thin film, the structure and magnetism are Studies in details.

2. EXPERIMENTAL DETAILS

The metallo-organic decomposition (MOD) method is exhibit oxygen atom as the heteroatom bridge between metal atoms and organic ligand [11]. These compounds are dissolved in appropriate solvent. The film are prepared by using this solution in require molar ratio. In this work Zinc 2-ethyl hexanoate and Nickel 2-ethyl hexanoate were used as Zn and Ni sources respectively. The syntheses of precursors used are described under following subsections.

2.1 Synthesis of Zinc-2-ethyl hexanoate $(C_7H_{15}COO)_2Zn$

To synthesize Zinc-2-ethyl hexanoate, 16ml of hexanoic acid was taken into 250 ml flask. In another flask 4 gm of KOH was dissolved in 30 ml distilled water to obtain the KOH solution. Two solutions were mixed to neutralize the hexanoic acid solution. The solution was allowed to stir constantly for about two hours. The solution appeared first milky and then clears on completion of neutralization. To this solution, 14.87 gm of Zinc Nitrate dissolved in about 50ml of distilled water was added and allowed to stir for another three hours. Zinc-2-ethyl Hexanoate gel was formed as a top layer. Gel was extracted with 40 ml of xylene from aqueous solution using separating funnel. Following chemical reaction occurred during the processing:

$$C_7H_{15}COOH + KOH \longrightarrow C_7H_{15}COOK + H_2O$$

$$2C_7H_{15}COOK + Zn(NO_3)_2 \longrightarrow 2KNO_3 + (C_7H_{15}COO)_2Zn$$

The solution was kept as a stock solution of Zinc.

2.2 Synthesis of nickel-2-ethyl hexanoate

To synthesize Nickel 2-ethyl hexanoate, 16 ml of hexanoic acid was taken into 250 ml flask. In another flask, 4 gm of KOH was dissolve in 30 ml distilled water to obtain the KOH solution. Two solutions were mixed to neutralize the hexanoic acid solution. The solution was allowed to stir

constantly for about two hours. The solution appeared first milky and then clears on completion of neutralization. To this solution, 7.2 gm of Nickel nitrate dissolved in about 50 ml of distilled water was added and allowed to stir for another three hours. Greenish colored, Nickel-2-ethyl hexanoate gel was formed as a top layer. Gel was extracted with 40 ml of xylene from aqueous solution using separating funnel. Following chemical reaction occurred during the processing:

$$C_7H_{15}COOH + KOH \longrightarrow C_7H_{15}COOK + H_2O$$

$$2C_7H_{15}COOK + Ni(NO_3)_2 \longrightarrow 2KNO_3 + (C_7H_{15}COO)_2Ni$$

The solution was kept as a stock solution of Nickel.

2.3 Thin film deposition by Spin coating

ZN films were prepared by dispensing a drop of metal organic solution on Si substrate, spin at the rate of 4500 rpm for 60sec using spin coating unit. These films were drying in muffle furnace at 350^{o}C for 5 minute. Drying and coating are sequentially repeated to get thickness of the film. As deposited ZN film are amorphous in nature. High temperature heat treatment is required to get crystalline film. These films were annealed at 550^{0}C temperature for three hour to crystallize. The crydtallization was done at the end of complete deposition of films. Fig 1 shows the schematic diagram for synthesis and film preparation by MOD.

3. RESULTS & DISCUSSIONS

3.1 XRD Results

The crystalline structure of the Ni doped ZnO thin films were analyzed by PHILIPS X-ray diffractometer. The diffraction patterns of nickel substituted Zinc Oxide thin film with different nickel concentration are shown in the Figs. 2 (a) to 2 (c), respectively for 2%, 4% and 7% nickel doping. All samples were annealed at 550^{o}C for three hour. It is confirmed that a polycrystalline wurtzite phase with c-axis preferred orientation is formed in all films. Slightly low intensity diffraction peaks may be attributed to secondary phase, implying that Ni atom might substitute for Zn atoms with minor secondary Phase formation.

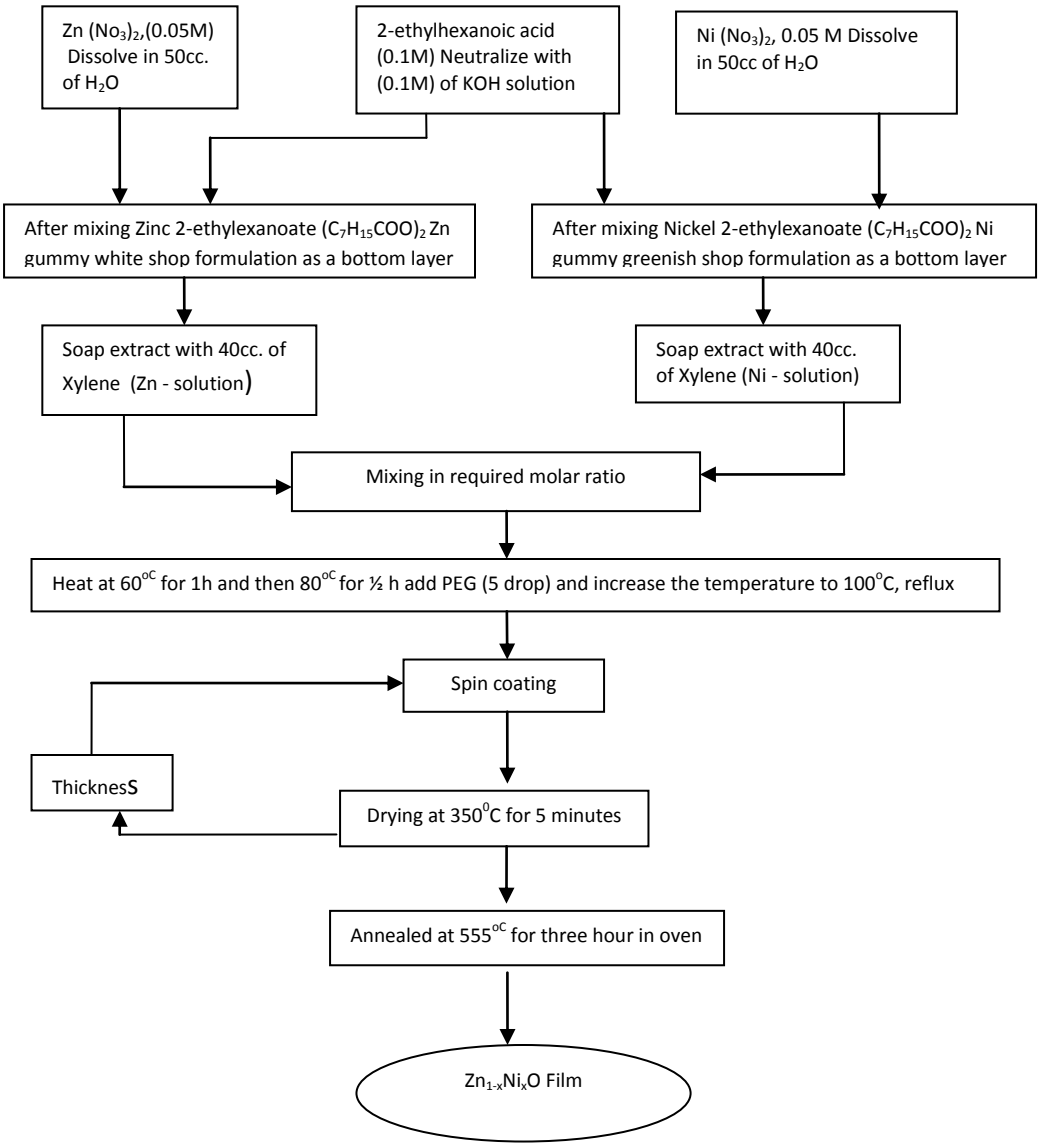

Fig. 1 Flow diagram of $Zn_{1-x}Ni_xO$ thin films by MOD method using spin coating technique.

Fig. 2(a) indicates that the XRD pattern of the ZN-02 thin film shows wurtzite hexagonal structure since diffraction lines such as (002), (102), and (110) at the diffraction angle $2\theta = 33^0$, $47^0$and 57^0 are the characteristics of the hexagonal structure. The intermediate phase has been found near diffraction angle $2\theta = 54^0$ and is marked as (*) in the pattern. These phases are usually present in the ZnO due to either Zn-Ni incomplete reaction or unreacted Ni in isolation on the surface of the films.

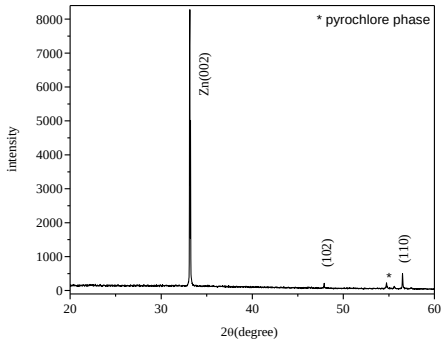

FIG. 2 (a). XRD pattern of $Zn_{0.98}Ni_{0.02}O$ thin film

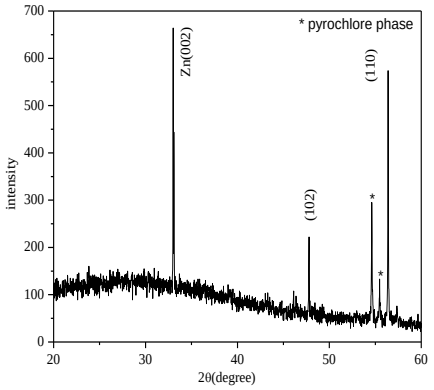

FIG. 2 (c). XRD pattern of $Zn_{0.93}Ni_{0.07}O$ thin film

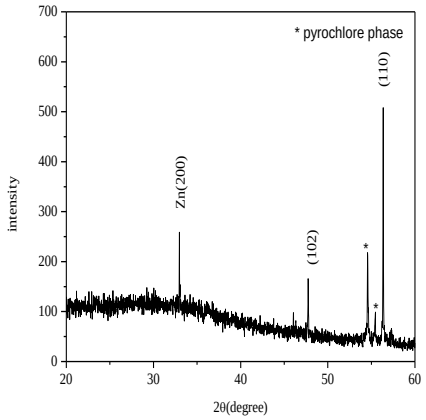

FIG. 2 (b). XRD pattern of $Zn_{0.93}Ni_{0.07}O$ thin film

The peaks (002) due to Zinc Oxide and peaks (102) and (110) are weak ZnO peaks due to slight Ni doping. In ZN-02 we get large intensity peak (002) and smaller peak (102) and (110) since Ni concentration is very small in ZN-02.

As concentration of Nickel increases to 4% in Fig. 2(b) (specimen ZN-04), there is a significant reduction in the intensity of (002) peaks. The intensity of (102), (110) peaks increased and intermediate phase near $2\theta = 54^0, 56^0$ formed on increasing Ni ions in deposited ZnO films.

On further increasing Ni concentration as in the Fig 3.4 (ZN-07) the intensity of (002) enhances and peaks (102), (110) and formation of intermediate phase also increases because of higher concentration of Ni concentration. From the Figs 2(a) to 2(c) it can be seen that the ZnO (002) peak position shifted

to lower angle side and *c*-axis lattice constant of the Ni-doped ZnO films decreases with the enhancement of the Ni- concentration. The result may be due to the substitution of Ni in ZnO.

The particles size in the specimen was calculated by Scherer's equation [12-13] using full width at half maximum. It is defined as full width of the peak at half maximum value and is important in calculating size of the grains/ particle in the specimen from the XRD diagram using the Scherer's equation. The full width at half maximum is very small for the ZN thin film. The Scherer's equation is given as:

$$t = 0.9\,\lambda / b\cos\theta$$

Where, t = particle size, b= FWHM, λ=Wave length of K_α line of Cu used in X-ray.

Serial No.	Composition ($Zn_{1-x}Ni_xO$)	Lattice constant c(A^0)	Lattice constant a (A^0)	c/a Ratio
1	$Zn_{0.98}Ni_{0.02}O$	5.391	3.244	1.632
2	$Zn_{0.96}Ni_{0.04}O$	5.382	3.262	1.620
3	$Zn_{0.93}Ni_{0.07}O$	5.344	3.308	1.615

Table 1 Lattice parameter ratio and crystal dimension in$Zn_{1-x}Ni_xO$ thin films

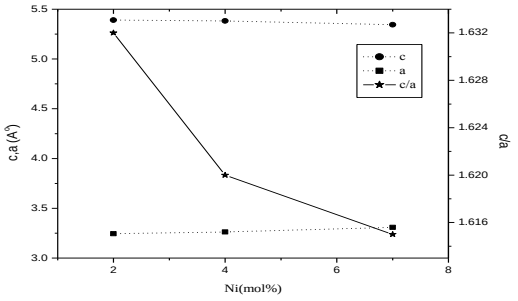

FIG. 3 Variation of c, a and c/a grain size in $Zn_{1-x}Ni_xO$ thin films with Ni concentration

The result shows that average particle size in specimen decrease as the concentration of Ni is increased. The value of lattice parameter and c/a ratio is given in table 1. The lattice parameter 'c' and 'c/a' value decrease continuously but the value of lattice parameter 'a' increases. Fig 3 shows variation of lattice constants c and a, and ratio value c/a with molar concentration of nickel in specimens. There is very smaller change in the c/a ratio, which means that there is slight distortion variation in the hexagonal structure.

3.2 Microstructure analysis

SEM has been used to investigate the detailed morphology and microstructure analysis of Ni–doped ZnO films and the possibility of precipitates, which might not be detected by XRD. The major interest here is to obtain smooth surface morphologies required for many device applications. When the particle are sufficiently uniform in size, they self assembled in closed packed, orderly grain particles super lattice. Microstructure evaluation in the film is relative of strong change in the composition and crystallization during annealing process.

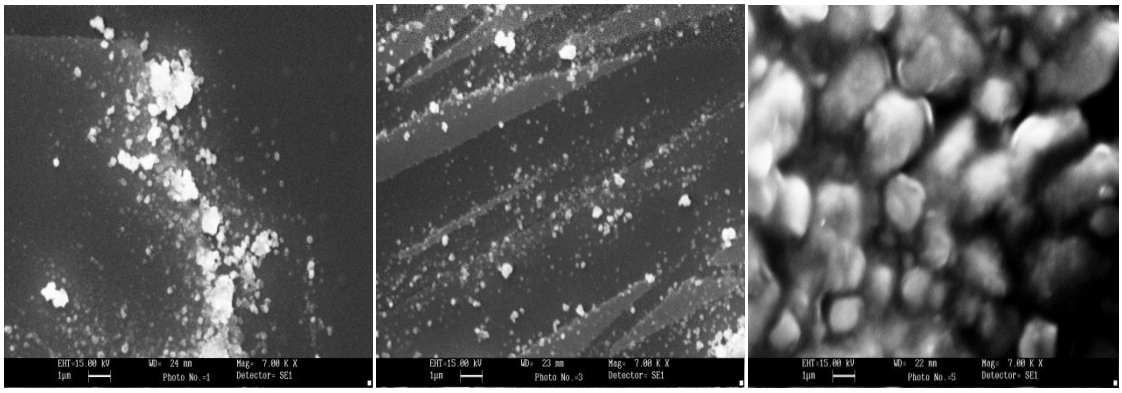

FIG. 4(a) SEM image of $Zn_{0.98}Ni_{0.02}O$, (b) $Zn_{0.96}Ni_{0.04}O$, (c) $Zn_{0.93}Ni_{0.07}O$ thin films.

Sr. no.	Compos-ition	Particle size XRD (nm)	Particle size SEM (nm)
1	ZN-02	270	278
2	ZN-04	198	199
3	ZN-07	320	327

Table 2 XRD & SEM particle size.

The investigation focuses on the crystalline morphology and dimension, grain size, grain boundaries and compactness of ZN film synthesized by MOD techniques. Figs 4(a) to 4(c) show surface morphology of the ZN film with different Ni contents. It is evident that surface of $Zn_{0.93}Ni_{0.07}O$ thin film is smooth without any cracks. Table 2 Show the comparison between of ZN particles size as measured from SEM and XRD and the graphical representation is also shown in Fig. 5.

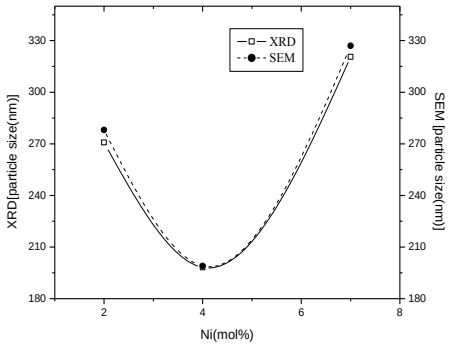

FIG. 5 SEM and XRD particle size in ZN thin film with different Ni concentration

3.3 Magnetic properties of $(Zn_{1-x}Ni_x)$ O thin film

The magnetic properties of ZN thin film were measured using Vibrating Sample magnetometer (model P 525) [14-15] and the result are shown in the Fig. 6(a) to Fig 6(b). Sufficient evidence for ferromagnetism (FM) at room temperature (RT) is emerged for ZN-07 thin films. The RT FM in our Ni-doped ZnO films could arise from a number of possible sources. Phase segregated NiO crystals are an unlikely source of this ferromagnetism because of the quantitative incorporation of dopants within the ZnO lattice in the DMS-QD precursors and because of the very low Curie temperatures. Metallic nickel precipitants are also unlikely candidates because such Ni precipitants were not observed in the structural analysis. We therefore conclude that the observed ferromagnetism is an intrinsic property of Ni^{2+}: ZnO thin film. Fig 6(a), ZN-02 film doesn't show ferromagnetic behavior and have very small magnetic moment. Since pure Zinc oxide did not exhibits magnetic behavior and concentration of Ni in ZN-02 is very low. The magnetic moment of pure Ni is 2 $\mu_{B.}$ So the magnetic moment of ZN-02 film is negligible.

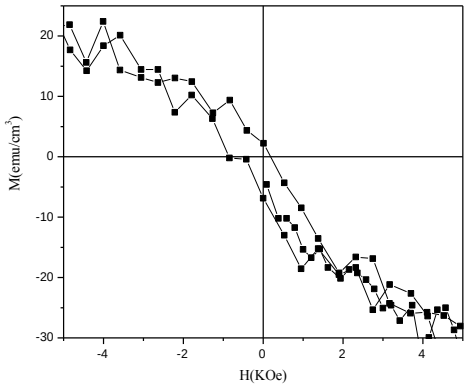

FIG. 6(a) M-H curve for $Zn_{0.98}Ni_{0.02}O$ thin film

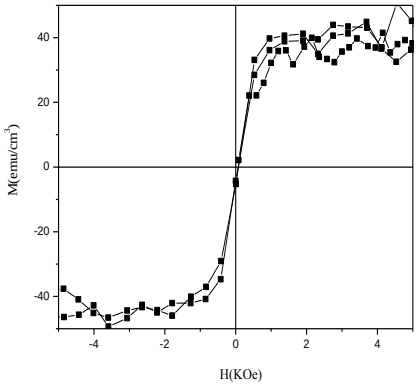

FIG. 6(c) M-H curve for $Zn_{0.93}Ni_{0.07}O$ thin film

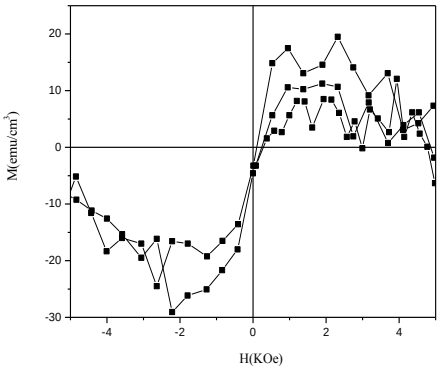

FIG. 6(b) M-H curve for $Zn_{0.96}Ni_{0.04}O$ thin film

4. CONCLUSION

In conclusion, Ni-doped ZnO ($Zn_{1-x}Ni_xO$, x = 0.02, 0.05, 0.07) diluted magnetic semiconductors thin films are prepared by sol–gel process. XRD analysis shows wurtzite structures for all the $Zn_{1-x}Ni_xO$ nanoparticles. With increasing Ni concentration, the wurtzite structures degrade gradually. The average value of particle size lies between 266-268 nm. The SEM image shows the homogeneous morphology with uniform grain formation in thin films. The ZN-07 (7% Ni doped ZnO thin film) has good homogeneity as compared to ZN-02 & ZN-04. Room temperature ferromagnetism has been observed in the $(Zn_{1-x}Ni_x)O$ thin films with 4 and 7% Ni doping concentration. The $(Zn_{0.93}Ni_{0.07})O$ thin film shows strong ferromagnetism with $M_s \sim 0.8\ \mu_B$ / Ni. The magnetic moment depends on Ni concentration and increases continuously as Ni concentration increases.

References

[1] J. M. D. Coey, M. Venkatesan and C. B. Fitzgerald, Donor impurity band exchange in dilute ferromagnetic oxides. *Nature Material*, 4, 173-179 (2005).

[2] K. Sato and H. Katayama-Yoshida. Material Design for Transparent Ferromagnets with ZnO-Based Magnetic Semiconductors, *J. Appl. Phys*, 39**,** L555- L558, (2000).

[3] Kimura H, Fukumura T, Kawasaki M, Inaba K, Hasegawa T and Koinuma H. , Rutile-type oxide-diluted magnetic semiconductor: Mn-doped SnO2. *Appl. Phys. Lett*, 80, 94-96, (2002).

[4] M. Venkatesan, C. B. Fitzgerald, J.G. Lunney, and J. M. D. Coey., Anisotropic Ferromagnetism in Substituted Zinc Oxide. *Phys. Rev. Lett*, 93**,** 177206-177209, (2004).

[5] Nguyen Hoa Hong and Joe Sakai., Ferromagnetic V-doped SnO2 thin films. *Physica. B*, 358, 265-268, (2005).

[6] Nguyen Hoa Hong, Antoine Ruyter, and W Prellier**.** Magnetism in Ni-doped SnO2 thin films. *J. Phys: Condens. Matter*, 17**,** 6533-6538, (2005).

[7] Nguyen Hoa Hong, Joe Sakai, W Prellier, and Awatef Hassini., Transparent Cr-doped SnO2 thin films: ferromagnetism beyond room temperature with a giant magnetic moment. *J. Phys: Condens. Matter.* 17, 1697-1702, (2005).

[8] S. B. Ogale, R. J. Choudhary, J. P. Buban, and S. R. Shinde., High Temperature Ferromagnetism with a Giant Magnetic Moment in Transparent Co-doped SnO2-δ.*Phys. Rev. Lett*, 91, 077205-077208, (2003).

[9] S. J. Pearton, C. R. Abernathy, M. E. Overberg, G.T. Thaler, D. P. Norton, N. Theodoropoulou, A. F. Hebard, Y. D. Park, F. Ren, J. Kim, and L. A. Boatner., Optical and magnetic properties of ZnO bulk crystals implanted with Cr and Fe. *J. Appl. Phys*, 93, 1-13, (2003).

[10] T. Dietl, H. Ohno, F. Matsukura, J. Cibert, and D. Ferrand., Optical and magnetic properties of ZnO bulk crystals implanted with Cr and Fe. *Science* , 287**,** 1019-1022, (2000).

[11] Y. X. Wang, Hui Liu, Z. Q. Li, X. X. Zhang, R. K. Zheng and S. P. Ringer., Role of structural defects on ferromagnrtism in amorphous Cr-doped ZnO films. *Appl. Phys. Lett*, 89, 042511-042513, (2006).

[12] Zhenjun Wang, Wendong Wang, Jinke Tang, Le Dung, Leonard Spinu, and Weilie Zhou., Electrical and ferromagnetic properties of Tb-doped indium–tin oxide films fabricated by sol–gel method. *J. Appl. Phys*, 83, 518-520, (2003).

[13] Coey, J.M.D., M. Venkatesan and C. P. Fitzgerald, Donor impurity band exchange in dilute ferromagnetic oxides. Nat. Mater., 4 173, (2005**)**.

[14] Dietl, T., H. Ohono, F. Matsukara, J. Cubert and D. Ferrand, Zener Model Description of Ferromagnetism in Zinc-Blende Magnetic Semiconductors. Science, 287 1019, (2000).

[15] Gosal, T., S. Kar and S. Chadhuri, Synthesis and optical properties of nanometer to micrometer wide hexagonal cones and columns of ZnO. J. cryst. Growth., 293 438, (2006).